ELSEVIER

Polymer 44 (2003) 2983–2991

polymer

www.elsevier.com/locate/polymer

The environment of lithium ions and conductivity of comb-like polymer electrolyte with a chelating functional group

Wu-Huan Hou[a], Chuh-Yung Chen[a,*], Cheng-Chien Wang[b]

[a]*Department of Chemical Engineering, National Cheng-Kung University, Tainan 70101, Taiwan, ROC*
[b]*Department of Chemical Engineering, Southern Taiwan University of Technology, Tainan 710, Taiwan, ROC*

Received 7 November 2002; received in revised form 31 January 2003; accepted 10 February 2003

Abstract

The behavior of lithium ions in a comb-like polymer electrolyte with a chelating functional group have been characterized by differential scanning calorimeter (DSC), dynamic mechanical analysis (DMA), Fourier transform infrared (FTIR) spectroscopy, ac impedance and ^{7}Li solid-state NMR measurements. The comb-like copolymer is synthesized by poly(ethylene glycol-methyl ether methacrylate) (PEGMEM) and (2-methylacrylic acid 3-(bis-carboxymethylamino) -2-hydroxy-propyl ester) (GMA-IDA). FTIR and ^{7}Li solid-state NMR spectra demonstrate the interactions of Li^{+} ions with both the ether oxygen of the PEGMEM and the nitrogen atom of the GMA-IDA segments. Moreover, ^{7}Li solid-state NMR shows that the lithium ions are preferentially coordinated to the GMA-IDA segment. The T_g increases for the copolymers doped with $LiClO_4$. These results indicate the interactions of Li^{+} with both PEGMEM and GMA-IDA segments form transient cross-links. The Vogel–Tamman–Fulcher (VTF)-like behavior of conductivity implies the coupling of the charge carriers with the segmental motion of the polymer chains. The dependence of the maximum conductivity on the composition of the copolymers and the doping lithium ion concentration was determined. The GMA-IDA unit in the copolymer improves the dissociation of the lithium salt, the mechanical strength and the conductivity.

Keywords: Polyelectrolyte; Chelating copolymer; Conductivity

1. Introduction

Solid polymer electrolytes (SPEs) have been extensively studied [1,2] since the discovery of ionic conduction in complexes of poly(ethylene oxide) (PEO) that contain alkali metal salts [3]. These ionic conductors can be used as polymer electrolytes in electrochemical devices [4]. Among these polyetectrolyte materials, PEO is the most thoroughly studied as a host for ions because PEO contains ether coordination sites and a flexible macromolecular structure, which assist the solvation of salts and promote ionic transport. Unfortunately, the ionic conductivity of the PEO-salt complex electrolyte is poor at room temperature because the ion transport above the glass transition temperature (T_g) depends on the segmental motion of polymer chains [2,5–7] and the semicrystallinity of PEO interferes with lithium ionic transport. The ionic conductivity of a polymer electrolyte is facilitated in elastomeric amorphous phases owing to segmental motion of the polymer chains [8]. Accordingly, much research has been devoted to synthesizing polymers with highly flexible backbones [9,10].

The polymeric electrolytes used in electric devices must satisfy several requirements, including high ionic conductivity, electrochemical stability, and superior mechanical properties. Thus, comb-like polymers with PEO side chains have recently attracted much interest [11–16]. These comb-like polymers possess the desired combination of structural strength and low T_g, such that greater segmental motion of the PEO side chains leads to increase mobility of the dissolved ions. The highest ambient temperature conductivity for comb-like polymer electrolytes is presently around 10^{-5} S cm^{-1}. However, the mechanical properties of these polymers are still not sufficient for them to serve as separators in lithium batteries.

Polar subunits, such as acrylamide, acrylonitrile, maleic anhydride, and carbonate, can be placed along the polymer

* Corresponding author. Tel.: +886-6-2757575; fax: +886-6-2360464.
E-mail address: ccy7@ccmail.ncku.edu.tw (C.Y. Chen).

0032-3861/03/$ - see front matter © 2003 Elsevier Science Ltd. All rights reserved.
doi:10.1016/S0032-3861(03)00135-6

chain as another strategy to increase the ionic conductivity of the polymer electrolytes and thereby to increase the dissociation of salt and the dielectric constant of the polymer host [17–19]. The polar subunits not only reduce the crystallinity of PEO but also coordinate the ions and thus increase the dissociation of lithium salt in SPE. The polar subunits significantly influence the lithium ion environment and ion transport. Solid-state NMR has been used to investigate the ionic structure and mobility of the charge carriers, and it yields insight into polymer-salt interactions in polymer electrolytes [20–25]. Moreover, ^{7}Li wide-line NMR and relaxation time measurements have been widely applied to elucidate the motion of the lithium ions and their interactions with polymer hosts, since the strong receptivity of ^{7}Li makes this nucleus very attractive to study. Although many researchers have concentrated on understanding the carrying species' transformation mechanism in SPEs, the interaction between the ion-polymer and the ion-salt, the nature of the charge carrier, and the ionic association process involved in ionic conductivity is still limited.

In the present study, a monomer (GMA-IDA) with strongly chelating functional group, glycidy methacrylate-iminodiacetic acid [26–28], is introduced into the comb-like PEO copolymer to promote dissociation of the lithium salt and increase both the free ion content and dielectric constant of the polymer electrolyte. Solid-state ^{7}Li NMR, differential scanning calorimeter (DSC), dynamic mechanical analysis (DMA) and Fourier transform infrared (FTIR) were employed to elucidate the interaction of lithium ions within both the PEO side chain and the chelating functional group segments of the copolymer doped with $LiClO_4$.

2. Experimental section

2.1. Synthesis of polyelectrolyte

Glycidyl methacrylate (GMA) (Aldrich Co.) was purified by distillation before used. Reagent-grade iminodiacetic acid (IDA) (Avocado Co.) and lithium hydroxide (LiOH) (Rdh Co.) were used without further purification. Glycidyl methacrylate was allowed to react with iminoidacetic acid lithium salt to produce the chelating monomer (2-methylacrylic acid 3-(bis-carboxymethylamino) -2-hydroxy-propyl ester)(GMA-IDA). This was copolymerized with poly(ethylene glycol) methyl ether methacrylate (PEGMEM) (Aldrich Co.).

The polymerization was conducted in a 500 ml four-necked round-bottom flask equipped with an anchor-propeller stirrer and nitrogen purge at 70 °C. Ammonium peroxodisulfate (APS; Showa) was used as an initiator. After 24 hr, the flask was cooled to ambient temperature. Copolymers of differing molar compositions of GMA-IDA/PEGMEM (10/90, 20/80, 30/70) were synthesized in a similar manner. Copolymers containing 10, 20, 30% molar ratio GMA-IDA were denoted as hybrid A, hybrid B, hybrid C, respectively.

2.2. Solution NMR experiments

High-resolution NMR measurements were performed on a Bruker AMX-400 spectrometer with ^{1}H and ^{13}C resonance frequencies at 400.13 and 100.61 MHz, respectively. The GMA-IDA monomer and copolymer was dissolved in deuterium oxide (D_2O). The ^{1}H and ^{13}C chemical shifts were referenced relative to tetramethylsilane (TMS) at 0.0 ppm.

2.3. DSC thermograms

Thermal analysis of the polymer electrolytes was carried out in a Dupont DSC 2910 differential scanning calorimeter with a heating rate 20 °C/min and a temperature range of −150 to 90 °C.

2.4. Dynamic mechanical analysis

The dynamic mechanical properties of the polymer electrolytes were measured in a Dupont DMA 2980 with a heating rate 5 °C/min and frequency 1 Hz at temperature range 40–290 °C.

2.5. Solid-state NMR measurements

^{7}Li MAS with power decoupling NMR spectra were recorded with a Bruker AVANCE-400 NMR spectrometer, equipped with a 7 mm double-resonance probe, operating at 400.13 MHz for ^{1}H and 155.5 MHz for ^{7}Li. Typical NMR experimental condition were as follow: $\pi/2$ pulse length, 4 μs; recycle delay, 30–150 μs; ^{1}H decoupling power, 65 kHz; spinning speed, 3 kHz. Chemical shifts were externally referenced to the solution LiCl at 0.0 ppm.

2.6. Infrared spectroscopy

FTIR spectra were recorded at room temperature using a Bio-Rad FTIR system coupled to a computer. The resolution and scan numbers of IR measurement were 2 cm^{-1} and 64 times, respectively. The spectra were collected over the range 700–4000 cm^{-1}.

2.7. Preparation of the composite electrolyte

The copolymer solution was mixed with different amounts of lithium perchlorate ($LiClO_4$; Fluka) in distilled water to obtain polymer electrolytes with various concentrations of $LiClO_4$. The solutions were cast onto a polypropylene plate, dried at 40 °C and then transferred to a vacuum oven for further drying at 60 °C for 5 days. The films were stored in an argon-filled drybox, maintained at a relative humidity of less than 2%, for further measurements.

The thickness of the films was controlled between 150 and 200 μm.

2.8. Impedance measurements

The ionic conductivity of the polymer electrolytes were obtained using an electrochemical cell consisting of the electrolyte film sandwiched between two stainless steel electrodes. The cell was placed inside an argon-filled thermostated oven and maintained at a relative humidity of less than 2%. Impedance analysis was recorded by using Autolab PGSTAT 30 equipment (Eco Chemie B.V., Netherlands) with the Frequency Response Analysis (FRA) system software under an oscillation potential of 10 mV from 100 kHz to 1 Hz in thermostated oven from 30 to 90 °C.

3. Results and discussion

3.1. Identification of the structures of monomer (GMA-IDA) and copolymer

The hydrophilic monomer with a chelating group (GMA-IDA) was prepared by the epoxidizing of glycidyl methacrylate (GMA) and iminodiacetic acid lithium salt (IDA-2Li). Fig. 1 shows the solution ^{1}H NMR spectrum of the GMA-IDA monomer in D_2O at room temperature. Table 1 lists the assigned chemical shifts in Fig. 1.

Copolymers with various compositions were synthesized by radical polymerization of PEGMEM with GMA-IDA. Fig. 2 compares the FTIR spectra of hybrid A, hybrid B and hybrid C. These spectra have peaks at 2875, 1730, and 1115 cm^{-1}, respectively, because all copolymers contain common units of $-CH_3$, carbonyl ester and $-CH_2-O-CH_2-$. Absorbance peaks at 3430 and 1630 cm^{-1} corresponding to $-OH$, and $-COO^-$ are also observed for all copolymers, and the intensity of the $-OH$ and $-COO^-$ stretching peaks increases with the GMA-IDA content. Solution ^{1}H NMR was used to identify the structure of hybrid B, as shown in Fig. 3. Table 1 also lists the assigned chemical shifts. The ^{1}H NMR spectra of hybrid A and hybrid C are similar to that of hybrid B. Both FTIR and NMR spectra reveal that a copolymer with a chelating group and PEG on the side chain has been successfully synthesized.

Table 1
Assignment of Solution ^{1}H NMR chemical shifts of GMA-IDA and hybrid B, where the structure of the repeat unit is shown as above

Chemical shift (ppm)	Assignment	Chemical shift (ppm)	Assignment
(a) ^{1}H NMR data of GMA-IDA			
6.13	H1	3.71–3.92	H4
5.71	H2	3.44–3.59	H5
4.75	D_2O	1.90	H6
4.20	H3		
(b) *^{1}H NMR data of hybrid B*			
4.75	D_2O	3.35	H3
4.15	H1	1.55–2.35	H5
3.44–3.95	H2 + H4	0.78–1.24	H6

3.2. Environment of lithium ions doped in polymer electrolytes

Scheme 1 depicts possible coordination of Li^+ ion to different groups in the hybrid polymers. Scheme 1(a)–(c)

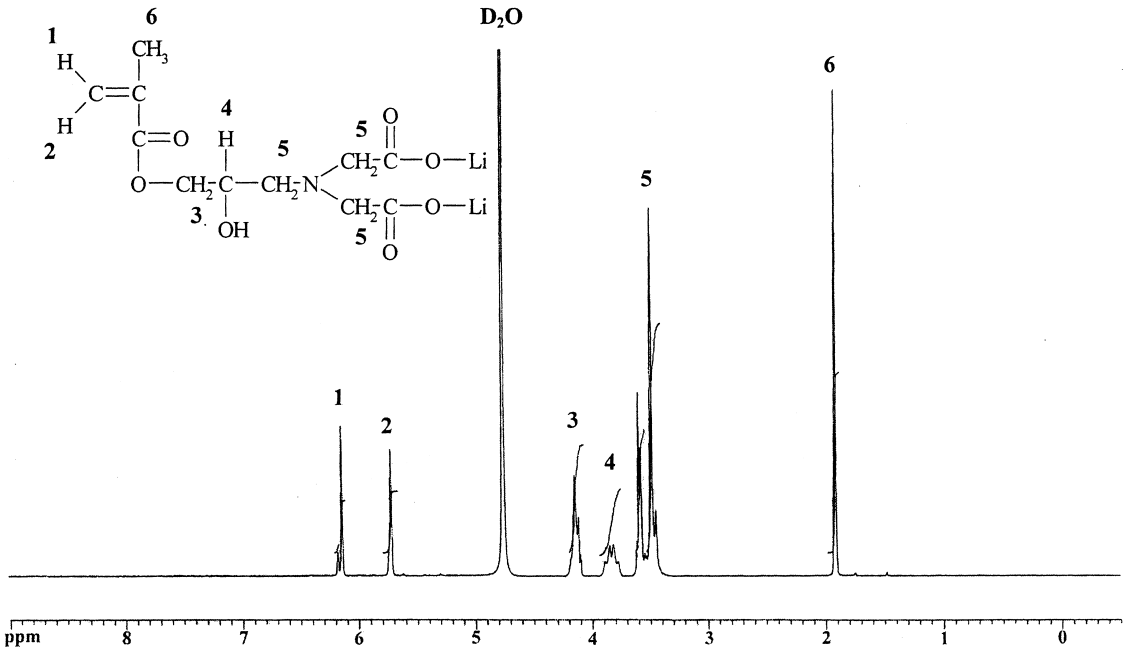

Fig. 1. ^{1}H high-resolution solution NMR spectra of GMA-IDA.

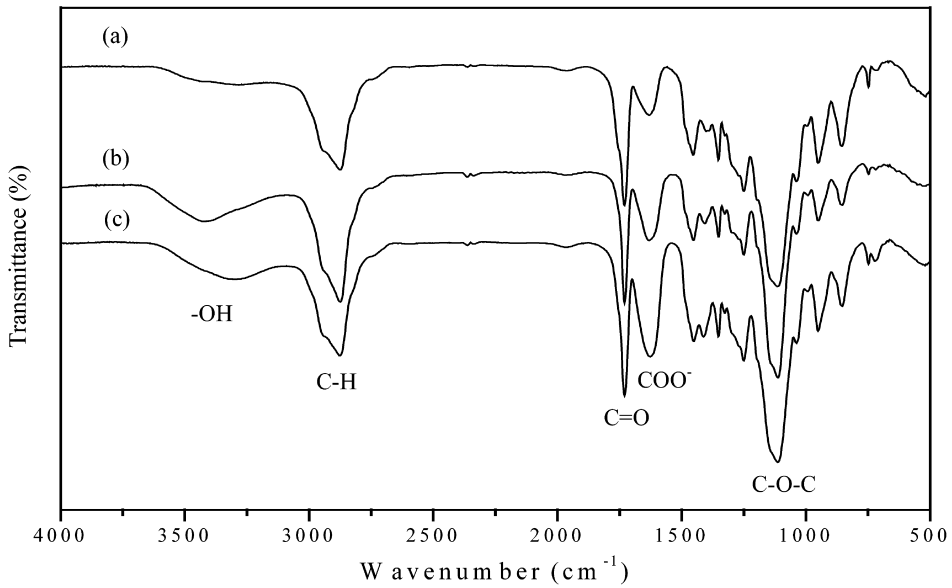

Fig. 2. FTIR spectra of composite copolymers: (a) hybrid A, (b) hybrid B, and (c) hybrid C.

indicates that Li^+ ions may interact, respectively, with the carbonyl, the N atoms of chelating groups, and/or the oxygen atom of the ether. FTIR spectra of these groups with various salt concentrations were compared to investigate the environment of the lithium ions. Fig. 4 presents the characteristics of the spectra for the C=O stretching region of the ester (1690–1840 cm^{-1}) (Scheme 1a) and the COO^- stretching region of the iminodiacetic acid (1540–1690 cm^{-1}) with various concentrations of $LiClO_4$. The IR spectra reveal no difference in the C=O stretching region but show significant changes in the COO^- stretching vibration. This is attributable to the interaction of the lithium ions with COO^- group of the iminodiacetic acid, but not with the C=O group of the ester (Scheme 1a). Therefore, the COO^- stretching region in this case may result from a change in the extent of ionization, due to the interaction of the lithium ions with the nitrogen atom of the chelating group (Scheme 1b). Furthermore, the attraction between the lone pair of electrons on the nitrogen atom and the COO^-Li^+ group reduces the ionization of the COO^-Li^+ group in hybrid B without doping with the lithium salt, as shown in Fig. 4a. Consequently, the absorbance band of the COO^- group shifts to a higher frequency. However, the coordination

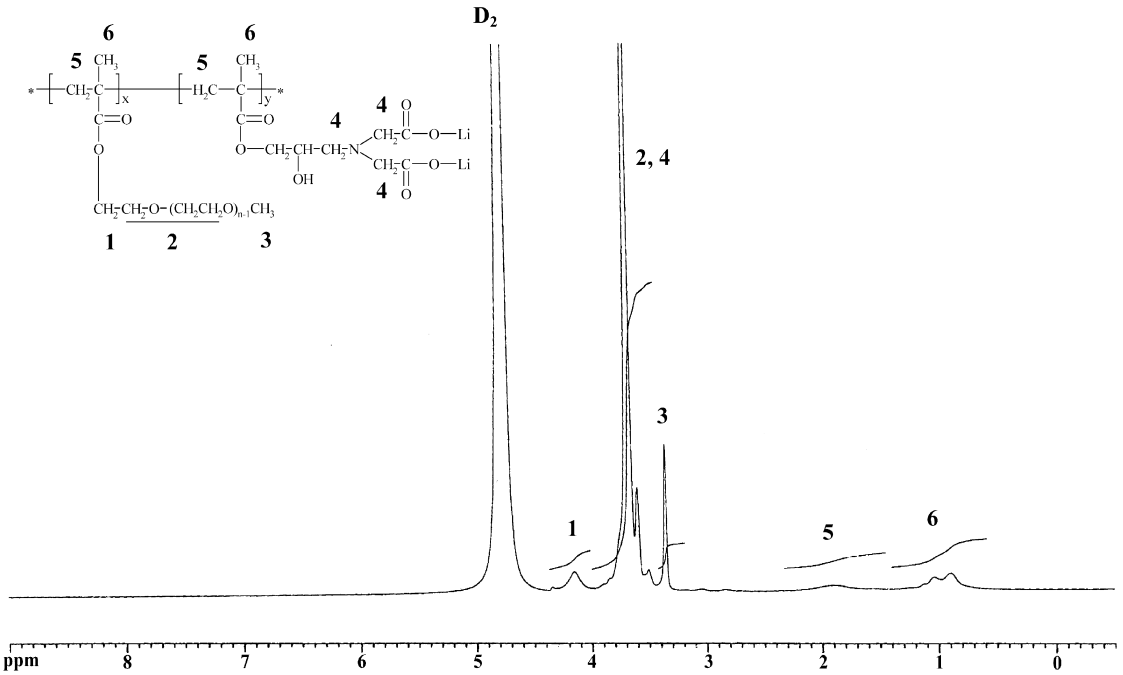

Fig. 3. ^1H high-resolution solution NMR spectra and the structure of the hybrid B.

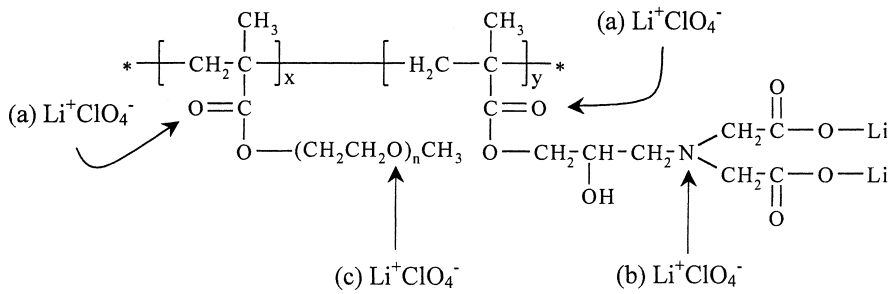

Scheme 1. Schematic representation of coordination of Li^+ ions to different positions: (a) to the carbonyl oxygens, (b) to the nitrogen atoms of chelated groups, and (c) to the ether oxygens.

between the lone pair of electrons on the nitrogen atom and the lithium ions reduces the attraction between the nitrogen atom and the COO^-Li^+ group after the lithium salt are doped in hybrid B (Figs. 4b–d). Thus, the increase in the ionization level of the COO^-Li^+ group shifts the COO^- band to a lower frequency. Fig. 5 shows the spectra corresponding to various concentrations of $LiClO_4$ in the ether oxygen stretching region (Scheme 1c). The absorbance band of the ether oxygen also shifts to a lower frequency as the salt concentration increases. This change in the stretching region of the ether oxygen can be expected because of the well-known coordination of the lithium ion to the un-bonded electrons of the ether oxygen, as has also been reported in another study [29].

^7Li magic angle spinning (MAS) NMR spectra for various $LiClO_4$ concentrations of copolymers, corresponding to the chelating group of GMA-IDA and the PEO side chain of PEGMEM, are examined and shown in Fig. 6. Fig. 6 displays high resolution ^7Li MAS NMR spectra to demonstrate the presence of three distinct Li^+ sites in the polymer electrolytes. As the temperature is reduced, three well resolved resonance peaks are observed at 0.26 ppm (site I), −0.22 ppm (site II), and −0.84 ppm (site III), respectively, with integrated intensities of approximately 0.5:0.3:0.2 are obtained at 203 K. Spinning sidebands are also observed at low temperatures, establishing that the ^7Li quadrupolar interaction is increased by a decrease in the lithium mobility as the temperature is reduced. Raising the temperature leads to shifts of these three resonance peaks, which eventually combine into a single resonance peak, as shown in Fig. 6. Whereas the classical peak merging involves a two-site exchange process, these three sites not only undergo a three-site exchange process, but probably also exhibit a temperature-dependent site preference [23, 30]. According to Wen et al. [23], the frequency of the jumps between the three sites must be greater than the separation of the three resonance peaks, since the peaks are observed at low temperatures. Thus the separation must exceed 100 Hz, for sites I, II and III to coalesce due to the increasing mobility of Li^+. At temperatures above 263 K, exchange is fast in comparison to the NMR time scale, resulting in a single resonance with a chemical shift that is the weight average of the individual components.

Fig. 7 shows the solid-state ^7Li NMR spectra for various salt concentrations, obtained at 203 K. As above, three distinct resonance peaks are observed and are well resolved in high amounts of the doped lithium salt. After deconvolution of hybrid B without the doped lithium salt in Fig. 7(a), two peaks, assigned as site I and site II, can be observed in the spectrum. The deconvolution of the low temperature spectra shows a Gaussian line for site I, whose line width is broader than a mixture of Lorentzian and Gaussian (1/1) line

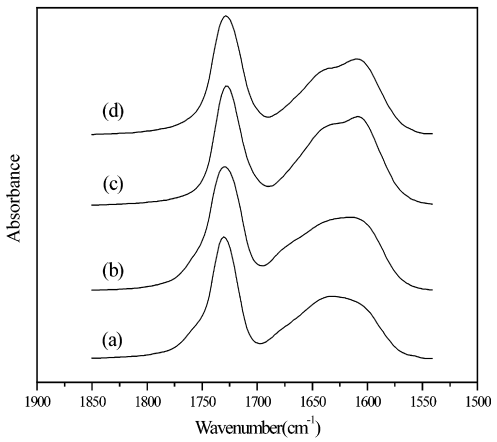

Fig. 4. FTIR spectra for −C=O and $-COO^-$ group region of composite copolymer hybrid B (copolymer with 20% GMA-IDA) with various $LiClO_4$ concentrations: (a) 0.0, (b) 0.5, (c) 1.5, and (d) 2.5 mmol/g of copolymer.

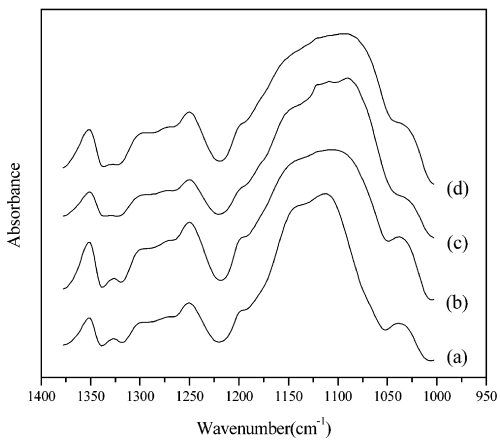

Fig. 5. FTIR spectra for −C−C−O-group region of composite copolymer hybrid B (copolymer with 20% GMA-IDA) with various $LiClO_4$ concentrations: (a) 0.0, (b) 0.5, (c) 1.5, and (d) 2.5 mmol/g of copolymer.

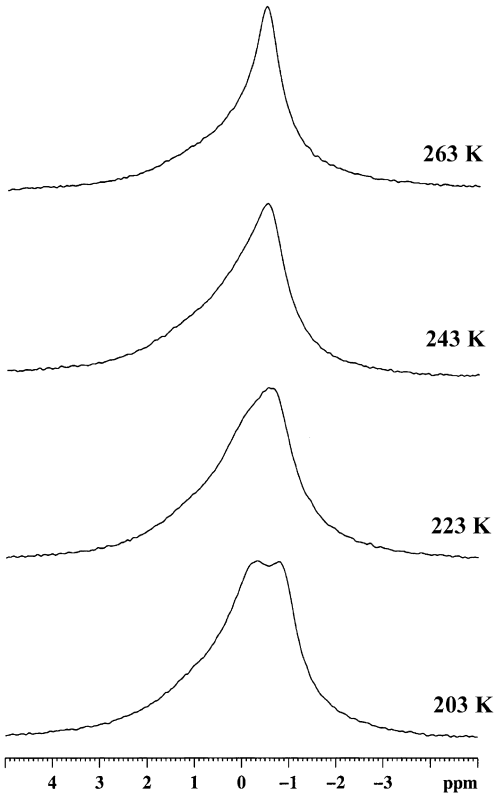

Fig. 6. Variable-temperature ^{7}Li proton-decoupled MAS NMR spectra of hybrid B doped with 0.5 mmol $LiClO_4$/g hybrid B.

for site II, implying that site II has more motional freedom than site I [23]. Site I is thus associated with the $COO^{-}Li^{+}$ group in the GMA-IDA segment. Site II is attributable to the coordination between nitrogen atom on GMA-IDA and lithium ions, which are dissociated from the $COO^{-}Li^{+}$ group of GMA-IDA. The increasing intensity for site II is attributed to the interaction between the nitrogen atom and the doped lithium salt. Notably, at doping concentrations of up to 0.2 mmol $LiClO_4$/g hybrid B, site III becomes visible and the intensity of site II significantly exceeds that of site III in Fig. 7b, indicating that the Li^{+} ion is preferentially coordinated to site II. The intensity of sites II and III increases with the concentration of the salt, as shown in Figs. 7c–e. The nitrogen atom on the chelating group interacts with the lithium ions more strongly than does the ether oxygen atom in the PEO side chain because of the higher donicity of the unpaired electron on the nitrogen. Moreover, site III is observed only after the lithium salt doping and both intensities of sites II and III depend on the salt concentration. Hence, site III is associated with the coordination between the ether oxygen atom in the PEO side chain and lithium ions.

In summary, the variable temperature ^{7}Li NMR spectra and the FTIR spectra represent an effective method for probing different local environments of the lithium ions in a polymer electrolyte. Such interactions of the lithium ions with the PEO side chain and chelating group are also evidenced by the DSC and DMA studies, described below.

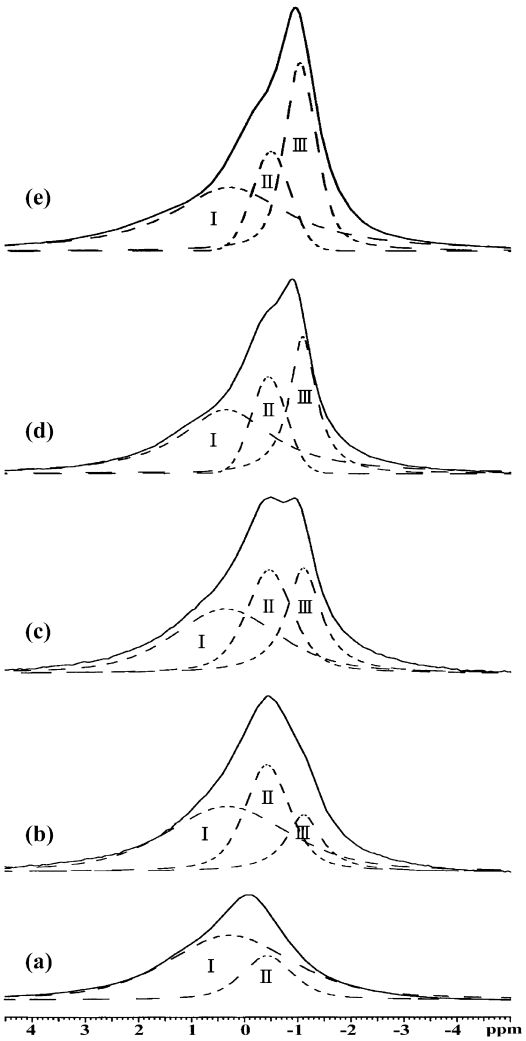

Fig. 7. Deconvolution of ^{7}Li proton-decoupled MAS NMR spectra at 203 K for hybrid B doped with (a) 0.0, (b) 0.2, (c) 0.5, (d) 1.0, and (e) 2.0 mmol $LiClO_4$/g hybrid B.

3.3. Thermal and dynamic mechanical properties

All the polymer electrolytes in this study are completely amorphous as judged by DSC analysis. DSC was also employed to elucidate the effect of $LiClO_4$ on the thermal transitions of the polyether side chain. The dissociation of alkali metal salts by polyethers has been reported to occur by coordination of the alkali metal ions with the ether oxygen of the polyethers, and many researchers [13,29,31,32] have studied the effect of such coordination on the T_g of the side chain. Different concentrations of $LiClO_4$ were added to hybrids A, B, C and the thermal properties are presented in Table 2. The T_g of PEO side chain increases with the concentration of the salt. According to other researchers [13,29,31,32], the increase in T_g is attributable to the inter- and intramolecular coordination of ether dipoles with the charge carriers, or dissociated ions, which may act as transient cross-link points between the lithium ions and the ether oxygen of the side chain. Additionally, the higher

Table 2
Thermal transition temperature of PEO side chain for lithium salt doped copolymer

[$LiClO_4$] (mmol/g of polymer)	T_g(°C)		
	Hybrid A	Hybrid B	Hybrid C
0.0	−58	−57	−57
0.5	−51	−50	−50
1.0	−41	−41	−40
1.5	−33	−35	−27
2.0	−27	−27	−15
2.5	−18	−20	0

Table 3
Thermal transition temperature of GMA-IDA segment for lithium salt doped copolymer

[$LiClO_4$] (mmol/g of polymer)	α-transition (°C)	
	Hybrid B	Hybrid C
0.0	217	227
0.5	228	260
1.0	238	274
1.5	251	277
2.0	257	279
2.5	262	279

T_g of the copolymer leads to slower local motion of the polyether segment, directly reducing the ionic mobility.

Effect of the salt concentration on the glass transition temperature of the GMA-IDA segment was identified by DMA analysis, which is more sensitive than DSC. Fig. 8 shows the dynamic mechanical spectra of hybrid B and Table 3 presents the corresponding results. DMA spectra of pure hybrid B (Fig. 8a) reveal that there are two transitions in the temperature range studied. One is the main glass transition (α-transition) temperature of the GMA-IDA segments, and the other is the β-transition temperature, which is lower than the α-transition temperature (T_α). Generally, the α- and β-transitions can be assigned to the main and side chain glass transition temperatures of the GMA-IDA segments. T_α increases and the intensity of β-transition decreases as the concentrations of $LiClO_4$ are increased, as shown in Fig. 8. The β-transition vanishes, however, at a doping level of 2.0 mmol $LiClO_4$/g hybrid B (Fig. 8e). The decrease in the β-transition intensity and increase in T_α may arise from the formation of the transient cross-linking between the lithium ions and the nitrogen atom of the GMA-IDA, which limit the local motion of the GMA-IDA segment. This result is similar to that for the T_g of the PEO side chain with various $LiClO_4$ concentrations.

A few interesting observations were made from the analysis of the T_g and T_α results for hybrid C. T_g and T_α of the parent polymer were normalized with the concentration

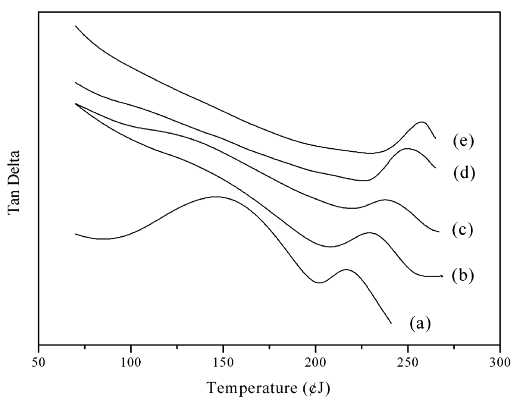

Fig. 8. DMA thermograms for hybrid B doped with various $LiClO_4$ concentrations: (a) 0.0, (b) 0.5, (c) 1.0, (d) 1.5, and (e) 2.0 mmol/g hybrid B.

of $LiClO_4$. Table 4 shows the $\Delta T_g/\Delta C$ and $\Delta T_\alpha/\Delta C$. $\Delta T_\alpha/\Delta C$ of the GMA-IDA segment is found to decrease with the concentration of the salt. At the initial $LiClO_4$ concentration, the lithium ions interact mainly with the GMA-IDA segment, enhancing the change in $\Delta T_\alpha/\Delta C$ of the GMA-IDA segment. However, above a $LiClO_4$ concentration of 0.5 mmol/g hybrid C, the amount of Li^+ chelated with GMA-IDA approaches saturation so the lithium ions may interact mainly with the polyether side chain. Consequently, the $\Delta T_g/\Delta C$ value of the polyether side chain at a high salt concentration far exceeds (Table 4) that at a low salt concentration. An attempt was also made to find the change in $\Delta T_\alpha/\Delta C$ and $\Delta T_g/\Delta C$ for hybrid B. However, unlike hybrid C, no obvious difference is noted since the GMA-IDA content in hybrid B is lower than that in hybrid C. Interaction of the lithium ions with the GMA-IDA segment and the polyether side chain was also demonstrated by the IR and NMR studies. The latter show that the lithium ions are preferentially coordinated to the GMA-IDA segment.

3.4. Salt concentration and ionic conductivity

Many researchers [13,29,31,32] have reported the ionic conductivity of comb-like polymer electrolytic systems. The temperature dependence of the ionic conductivity of the polymer electrolytes is found to be well represented by a Vogel–Tamman–Fulcher (VTF) type equation, since the ion mobility is coupled with the segmental motion of the

Table 4
Thermal transition temperature of PEO side chain and GMA-IDA segment for lithium salt doped copolymer

[$LiClO_4$] (mmol/g of polymer)	Hybrid B		Hybrid C	
	$\Delta T_g/\Delta C$	$\Delta T_\alpha/\Delta C$	$\Delta T_g/\Delta C$	$\Delta T_\alpha/\Delta C$
0.0	–	–	–	–
0.5	14.0	22.0	14.0	66.0
1.0	15.0	21.0	17.0	47.0
1.5	14.0	22.7	20.0	33.3
2.0	14.5	20.0	21.0	26.0
2.5	14.4	18.0	22.8	20.8

polymer chain,

$$\sigma = AT^{-1/2}\exp\left(\frac{-B}{K_b(T - T_0)}\right) \quad (1)$$

where A is a constant proportional to the number of carrier ions; B is the pseudo-activation energy related to the motion of the polymer segment, K_b is the Boltzmann constant, and T_0 is a reference temperature, normally associated with the ideal T_g at which the free volume is zero or with the temperature at which the configuration entropy becomes zero [25]. Fig. 9 shows the ionic conductivity (σ) at 30 °C for the comb-like polymer electrolytes, complexed with $LiClO_4$ at several concentrations. The ionic conductivity increases, passes a maximum, and then decreases, as the salt concentration is increased. As reported by Nishimoto et al. [15] the ionic conductivity is proportional to the product of the number of charge carriers and their mobility. On the basis of the previous discussions, T_g increases with the salt concentration. The increase in T_g not only reduces the segmental motion of the polymer electrolytes but also directly reduces the ionic mobility. However, the number of the charge carriers increases with the salt concentration. Consequently, the maximum value of ionic conductivity, as shown in Fig. 9, is determined by these two opposing effects. The highest conductivity at 30 °C is 1.1×10^{-5} S cm^{-1}, for hybrid A doped with 2.0 mmol $LiClO_4$/g hybrid A, and this conductivity is higher than 10^{-7}–10^{-8} S cm^{-1} for conventional PEO-based electrolytes [3,4] and -10^{-6} S cm^{-1} for another comb-like copolymer [13,29]. The results have established the possibility of improving the ionic conductivity by increasing the polarity of the polymer host, and thus increasing the number of charge carriers.

On the other hand, Fig. 10 plots the $\log(\sigma T^{1/2})$ data for the electrolyte samples against reciprocal temperature, to show that the variation in conductivity with temperature follows the VTF relationship. This indicates the coupling of the charge carriers with the segmental motion of the polymer chain and the ionic conductivity change is dominated by the change in ionic mobility, as predicted by the free volume theory.

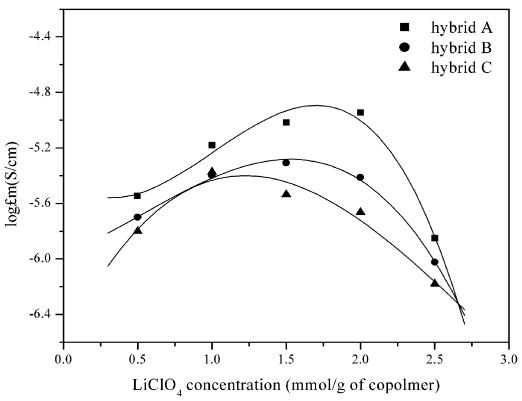

Fig. 9. Ionic conductivity vs $LiClO_4$ concentration for all polymer electrolytes at 30 °C.

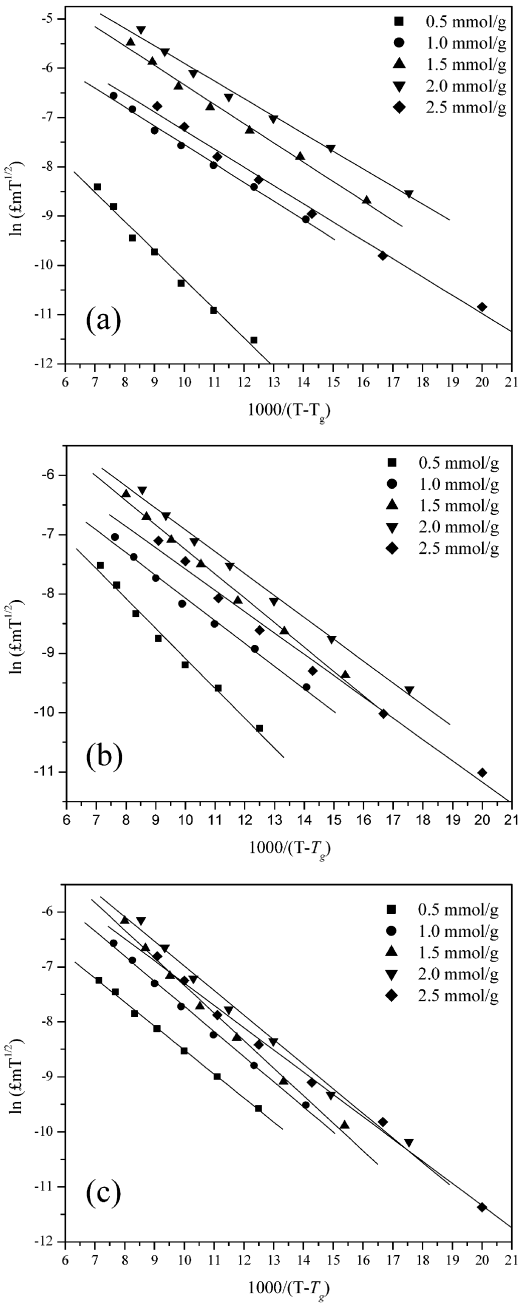

Fig. 10. VTF plots of ionic conductivity for composite polymer electrolytes complexed with $LiClO_4$: (a) hybrid A, (b) hybrid B, and (c) hybrid C.

4. Conclusions

A polymer electrolyte synthesized from PEGMEM and GMA-IDA complexed with $LiClO_4$, reveals a significant interaction of the lithium ions with the polyether side chain and the chelated group on the GMA-IDA segment. ^{7}Li MAS NMR was used to characterize the different local environments of the lithium ions and shows that the lithium ions are

preferentially coordinated to the GMA-IDA segment in the polymer electrolytes. As a consequence of this interaction, both T_g of the polyether side chain and of the GMA-IDA segment increases with the salt concentration. The maximum conductivity measured in this study exceeds the values reported in the literature [13,29]. The results establish that increasing the chelating group in the polymer host will increase the content of the charge carriers, and thus improves the conductivity of the polyelectrolyte.

Acknowledgements

The financial support of this research by the National Science Council of the Republic of China under Contract No. NSC90-2216-E-006-026- is gratefully acknowledged. The authors highly appreciated Ms Ru-Rong Wu for her profound contribution in NMR experiments.

References

[1] Gray FM. In: Vincent CA, MacCallum JR, editors. Polymer Electrolytes Reviews. London: Elsevier Applied Science; 1987.
[2] Gray FM. Solid Polymer Electrolytes, Fundamentals and Technological Applications. New York: VCH; 1991.
[3] Fenton DE, Parker JM, Wright PV. Polymer 1973;14:589.
[4] Wright PV. Br Polym J 1975;7:319.
[5] Killis A, LeNest JF, Cheradame H, Gandimi A. Makromol Chem 1982;183:2835.
[6] Druger SD, Nitzan A, Ratner MA. J Chem Phys 1983;79:3133.
[7] Ratner MA, Shriver DF. Chem Rev 1988;88:109.
[8] Magistris A, Singh K. Polym Int 1992;28:277.
[9] Sylla S, Sanchez JY, Armand M. Electrochim Acta 1992;37:1699.
[10] Alamgir M, Moulton RD, Abraham KM. In: Abraham KM, Salomon M, editors. Primary and Secondary Lithium Batteries. Pennington, NJ: The Electrochemical Society; 1991. p. 131.
[11] Xia DW, Smid J. J Polym Sci, Polym Lett Ed 1984;22:173.
[12] Cowie MG, Martin CS, Firth AM. Br Polym J 1988;20:247–52.
[13] Gnanaraj JS, Karekar RN, Skaria S, Rajan CR, Ponrathnam S. Polymer 1997;38(14):3709–12.
[14] Qi L, Lin Y, Jing X, Wang F. Solid State Ionics 2001;139:293–301.
[15] Nishimoto A, Agehara K, Furuya N, Watanabe T, Watanabe M. Macromolecules 1999;32:1541–8.
[16] Ikeda Y, Wada Y, Matoba Y, Murakami S, Kohjiya S. Electrochim Acta 2000;45:1167–74.
[17] Xu K, Zhou T, Deng ZH, Wan GX. Chin J Polym Sci 1992;10:223.
[18] Forsyth M, Tipton AL, Shriver DF, Ratner MA, MacFarlane DR. Solid State Ionics 1997;99:257.
[19] Xu W, Belieres JP, Angell CA. Chem Mater 2001;13:575–80.
[20] Kim CH, Park JK, Kim WJ. Solid State Ionics 1999;116:53.
[21] Mustarelli P, Quartarone E, Capiglia C, Tomasi C, Magistris A. Solid State Ionics 1999;122:285.
[22] Ng STC, Forsyth M, MacFarlane DR, Garcia M, Smith ME, Strange JH. Polymer 1998;39:6261.
[23] Wang HL, Kao HM, Wen TC. Macromolecules 2000;33:6910–2.
[24] Forsyth M, Jiazeng S, MacFarlane DR. Electrochim Acta 2000;45:1243.
[25] Wang HL, Kao HM, Digar M, Wen TC. Macromolecules 2001;34:529–37.
[26] Wang CC, Chang CC, Chen CY. Macromol Chem Phys 2001;202:882–90.
[27] Wang CC, Chen CY. J Appl Polym Sci 2002;85:919–28.
[28] Wang CC, Chen CY, Chang CC. J Appl Polym Sci 2002;84:1353–62.
[29] Gnanaraj JS, Karekar RN, Skaria S, Ponrathnam S. Bull Electrochem 1996;12:738–42.
[30] Abragam A. The Principle of Nuclear Magnetism. Oxford: Oxford University Press; 1961.
[31] Nishimoto A, Watanabe M, Ikeda Y, Kohjiya S. Electrochim Acta 1998;43:1177–84.
[32] Watanabe M, Endo T, Nishimoto A, Miura K, Yanagida M. J Power Sources 1999;81–82:786–9.